Robotica (2000) volume 18, pp. 59–70. Printed in the United Kingdom © 2000 Cambridge University Press

On the Liapunov stability of multi-finger grasps

Mikhail Svinin,* Kanji Ueda* and Makoto Kaneko**

SUMMARY

This paper deals with the stability of a rigid body under multiple contact forces. First, the problem is considered at the force planning level, and the stability of a force distribution is formulated. For this problem, the stiffness tensor is derived, and its basic properties are analyzed. Necessary and sufficient conditions for stability of a force distribution are established in an analytical form. These conditions, considered under unilateral frictional constraints, are studied on an illustrative example. Next, it is shown that stabilization of an unstable force distribution can be done by a simple control law. The stability conditions for this control law are formulated by transforming the stiffness tensor to the center of stiffness. Finally, conclusions on the contradiction between the Liapunov stability and the contact stability of the objects are drawn.

KEYWORDS: Multi-finger grasp; Stability analysis; Stiffness tensor; Force redundancy; Internal forces; Friction.

1. INTRODUCTION

One of the fundamental problems in controlling multi-fingered hands is the stability of the resulting grasp. In recent years, the problem has been addressed from different points of view, and a number of approaches to define grasping stability and its relation to concepts such as grasping form and force closure, have been proposed in the literature. Good surveys of this topic can be found in references 1 and 2.

In the research community, stability of a grasp is understood in two ways.[3] One is that of force-closure, and the other is based on the classical Liapunov's definition of stability. The former approach relates to the ability to resist an arbitrary force/moment, while the latter relates to the ability to return to an equilibrium when displaced from it. The force-closure-based definition is essentially static, while the Liapunov's definition is dynamic, or better say energetic as it requires examining the potential energy at equilibrium. This paper deals with the stability understood in the Liapunov's sense.

In literature, the finding of stable grasping configurations by minimizing the potential energy stored in elastic fingers is shown,[4] and a general model of the compliance of multi-finger grasps is developed.[5] An approach for constructing three-dimensional stable grasps, where each finger is replaced by virtual springs, is presented in reference 6. Using this approach and ignoring gravity and external forces, conditions for the stability of a planar grasp are derived in an analytical form.[7]

The stability analysis is conducted under a special arrangement of virtual springs.[7] More accurate and detailed derivation of the stiffness matrix of the object is given in reference 8, where the results are presented for the three dimensional case. No special arrangements for the virtual springs is necessary since the stiffnesses of the virtual springs are introduced through the finger-tip position feedback. Similar framework for studying grasping stability is explored in reference 9. Contact geometry is introduced into the stability analysis in references 10–13. The gravitational effects in the stability problem are investigated in references 3 and 14.

Basically, the total stiffness of an object grasped by multiple fingers has two sources: the first one is due to the compliance of the fingers, while the second is due to the contact force interaction between the fingers and the object. Roughly, the Cartesian stiffness of the fingers is defined by the transformation of the joint stiffness to the Cartesian level through the finger Jacobian. The Cartesian stiffness of the fingers is symmetric and positive definite (and therefore stable) as long as the joint stiffness matrix is symmetric and stable.

On the other hand, the stiffness due to the contact force interactions is not necessarily positive definite. It depends on the contact force distribution, and is often the source of grasping instability. In the most simple form it can be shown on the flipping coin example.[15] It should be noted that a similar subject—stability due to internal forces in mechanisms with closed kinematic chains—is analyzed in references 16 and 17.

One possible approach to provide stable grasping is based on decomposition of the total stiffness, and designing the corresponding matrices, the Cartesian finger stiffness and the stiffness due to the contact forces, separately. Indeed, if they are both stable, then the resulting stiffness will also be stable. If, however, the contact-force-induced stiffness cannot be made stable the design of the Cartesian finger stiffness becomes complicated. Thus, the design of the contact force distribution is a very important part of the solution to the stability problem.

Our work is motivated mainly by the reference[18] where the rotational stability of the grasped object under the constant contact forces is analyzed from the classical standpoint of the Liapunov's theory. However, the relation between the stability and the force distribution has not been studied in detail. Furthermore, the necessary and sufficient conditions for the stability have not been obtained in an analytical form. All this, taken together, sets the goals for

* Mechanical Engineering Department, Kobe University, Rokkodai, Nada-ku, Kobe 657-8501 (Japan)
E-mail: svinin@mech.kobe-u.ac.jp
** Robotics Laboratory, Department of Industrial and System Engineering, Hiroshima University, 1-4-1, Kagamiyama, Higashi-Hiroshima 739-8527 (Japan)
E-mail: kaneko@huis.hiroshima-u.ac.jp

https://doi.org/10.1017/S0263574799002465 Published online by Cambridge University Press

this paper---to relate the force distribution to the stability, and to obtain the stability conditions.

This paper is organized as follows. In Section 2, an analytical expression for the stiffness tensor is derived, and a definition of the stable force distribution is given. Necessary and sufficient conditions for stability of the force distribution are derived in Section 3. The topic of stability analysis is treated in Section 4. The stability conditions under unilateral frictional constraints are studied in Section 5 on an illustrative example. Section 6 discusses stabilization of an unstable force distribution. Comments on the relation between the Liapunov stability and the contact stability of the object are given in Section 7. Finally, conclusions are presented in Section 8.

2. STABLE FORCE DISTRIBUTION

Consider a rigid body subjected to multiple frictional contacts. Assume that constant forces $\boldsymbol{f}_1, \boldsymbol{f}_2, \ldots, \boldsymbol{f}_n$ are applied at the points defined by the radius-vectors $\boldsymbol{\rho}_1, \boldsymbol{\rho}_2, \ldots, \boldsymbol{\rho}_n$ drawn from the center of mass O. The dynamic equations read

$$m\ddot{\boldsymbol{x}} = m\boldsymbol{g} + \sum_{i=1}^{n} \boldsymbol{f}_i, \quad \boldsymbol{J}\dot{\boldsymbol{\omega}} + \boldsymbol{\omega} \times \boldsymbol{J}\boldsymbol{\omega} = \sum_{i=1}^{n} \boldsymbol{\rho}_i \times \boldsymbol{f}_i, \qquad (1)$$

where $\dot{\boldsymbol{x}}$ and $\boldsymbol{\omega}$ are the quasi-coordinates, m is the mass of the body, $\boldsymbol{J}$ is the inertia tensor, and $\boldsymbol{g}$ is the gravity vector. Since the contact forces are assumed to be constant, linearizing (1) at the equilibrium ($\dot{\boldsymbol{x}} = 0$ and $\boldsymbol{\omega} = 0$) gives

$$m\Delta\ddot{\boldsymbol{x}} = \sum_{i=1}^{n} \Delta\boldsymbol{f}_i, \quad \boldsymbol{J}\ddot{\boldsymbol{\theta}} + \boldsymbol{K}\boldsymbol{\theta} = \sum_{i=1}^{n} \boldsymbol{\rho}_i \times \Delta\boldsymbol{f}_i, \qquad (2)$$

where $\boldsymbol{\theta}$ is the vector of infinitesimal rotation of the body, and

$$\boldsymbol{K} = \sum_{i=1}^{n} (\boldsymbol{\rho}_i^{\mathrm{T}} \boldsymbol{f}_i)\boldsymbol{I} - \boldsymbol{\rho}_i \boldsymbol{f}_i^{\mathrm{T}} \qquad (3)$$

is the stiffness tensor. Note that in the planar case the rotational stiffness is a scalar given by

$$\boldsymbol{K} = \sum_{i=1}^{n} \boldsymbol{\rho}_i^{\mathrm{T}} \boldsymbol{f}_i. \qquad (4)$$

The following properties of the stiffness tensor can be formulated directly.

(i) The stiffness tensor does not depend on the location of the origin of the reference frame. That is if we change the origin from O to O' the matrix $\boldsymbol{K}$ still will be defined by (3) with $\boldsymbol{\rho}_i$ drawn from O. The proof is straightforward and is omitted here due to the page limitation.

(ii) $\boldsymbol{K}$ is symmetric as long as the object is at equilibrium. Indeed, one can prove that $\boldsymbol{K} - \boldsymbol{K}^{\mathrm{T}} = \boldsymbol{\Omega}(\sum_{i=1}^{n} \boldsymbol{\rho}_i \times \boldsymbol{f}_i)$. Therefore, the skew-symmetric part of $\boldsymbol{K}$ is always zero by the static equations. Here, $\boldsymbol{\Omega}$ is the skew-symmetric operator such that $\boldsymbol{\Omega}(\boldsymbol{a})\cdot\boldsymbol{b} \equiv \boldsymbol{a} \times \boldsymbol{b}$.

(iii) The stiffness $\boldsymbol{K}$ defines the potential energy of the constant contact forces $\boldsymbol{f}_i$. Note that even if the contact moments $\boldsymbol{m}_i$ (such as those used in the "soft" finger contact models) were present in (1), they would not enter the stiffness tensor. However, the contact moments would make the system nonconservative because in this case $\boldsymbol{K} - \boldsymbol{K}^{\mathrm{T}} = -\boldsymbol{\Omega}(\sum_{i=1}^{n} \boldsymbol{m}_i)$. Therefore, the stiffness matrix would become asymmetric and its eigen-values would be complex numbers unless the nonconservative curl, $\sum_{i=1}^{n} \boldsymbol{m}_i$, is zero.

(iv) The stiffness tensor $\boldsymbol{K}$ is not always and not necessarily positive definite. The judgment on the positive definiteness of $\boldsymbol{K}$ can be done easily only for some simple cases of force loading. Consider, for example, the case when all the applied forces are co-planar to the correspondent vectors $\boldsymbol{\rho}_i$, i.e., $\boldsymbol{f}_i = k_i \boldsymbol{\rho}_i$. Formula (3) gives

$$\boldsymbol{K} = \sum_{i=1}^{n} k_i \left\{ (\boldsymbol{p}_i^{\mathrm{T}} \boldsymbol{p}_i)\boldsymbol{I} - \boldsymbol{p}_i \boldsymbol{p}_i^{\mathrm{T}} \right\} \qquad (5)$$

As can be seen, $\boldsymbol{K}$ has the structure of the inertia tensor of a system of points built on the vectors $\boldsymbol{\rho}_i$, with k_i playing the role of masses. Therefore, if all $k_i \geq 0$, i.e., all the forces are stretching, $\boldsymbol{K}$ is positive definite. In the opposite case, when all $k_i \leq 0$, i.e., all the forces are compressive, $\boldsymbol{K}$ is negative definite.

However, in the general case, when k_i have different signs or when the applied forces $\boldsymbol{f}_i$ are not co-planar to $\boldsymbol{\rho}_i$, it is not that easy to make judgment on the properties of $\boldsymbol{K}$ without direct computations.

Now, consider (2) with $\Delta\boldsymbol{f}_i = 0$ (no feedback). In doing so, the grasp is considered on the position/force planning level. The translational part of (2) is not influenced by forces, and is out of interest at the force planning level. On the other hand, the rotational part of (2) depends on the force distribution, and its stability can be judged by $\boldsymbol{K}$. In this situation, being at the force planning level, it is meaningful to talk about stability of the force distribution. In what follows, a particular force distribution scheme will be called unstable if $\boldsymbol{K}$ is negative definite, and stable otherwise. The reason for taking this view is simple—even if the contact-force-induced stiffness matrix $\boldsymbol{K}$ is positive semi-definite, the resulting stiffness of the object can be easily made stable with simple proportional control of the finger joints.

3. STABILITY CONDITIONS

In general, the judgement on the positive definiteness of the matrix $\boldsymbol{K}$ can be done in terms of its eigen-values. The eigen-values can be easily calculated in numbers. However, they cannot be represented in a convenient, analytical form. Therefore, other invariants of $\boldsymbol{K}$ should be established to conduct the stability analysis in an analytical form.

https://doi.org/10.1017/S0263574799002465 Published online by Cambridge University Press

To obtain the stability conditions for the matrix $\boldsymbol{K}$, consider the characteristic equation

$$\det(\boldsymbol{K} - \lambda \boldsymbol{I}) = 0. \tag{6}$$

Let $\boldsymbol{R} = \{\boldsymbol{\rho}_1, \boldsymbol{\rho}_2, \ldots, \boldsymbol{\rho}_n\}^{\mathrm{T}}$, $\boldsymbol{R} \in \mathbb{R}^{3\times n}$, and $\boldsymbol{F} = \{\boldsymbol{f}_1, \boldsymbol{f}_1, \ldots, \boldsymbol{f}_n\}^{\mathrm{T}}$, $\boldsymbol{F} \in \mathbb{R}^{3\times n}$. Note that the eigenvalues of the matrix $\boldsymbol{K}$ are related to the eigenvalues of the matrix $\boldsymbol{R}\boldsymbol{F}^{\mathrm{T}} = \sum_{i=1}^{n} \boldsymbol{\rho}_i \boldsymbol{f}_i^{\mathrm{T}}$ as

$$\lambda(\boldsymbol{K}) = L - \lambda(\boldsymbol{R}\boldsymbol{F}^{\mathrm{T}}), \tag{7}$$

and the characteristic equation (6) can be written down in the following form

$$(L-\lambda)^3 - L(L-\lambda)^2 + S(L-\lambda) - V = 0. \tag{8}$$

Here, L, S, and V are the sums of the principal minors—of the 1st, 2nd and 3rd order, respectively—of the matrix $\boldsymbol{R}\boldsymbol{F}^{\mathrm{T}}$. Using the Cauchy-Binet theorem,[19] the principal minor of the p-th order of the matrix $\boldsymbol{R}\boldsymbol{F}^{\mathrm{T}}$ is given by

$$\boldsymbol{R}\boldsymbol{F}^{\mathrm{T}}\begin{pmatrix} i_1 \ldots i_p \\ i_1 \ldots i_p \end{pmatrix} = \sum_{1\le k_1 < \ldots < k_p \le n} \boldsymbol{R}\begin{pmatrix} i_1 \ldots i_p \\ k_1 \ldots k_p \end{pmatrix} \boldsymbol{F}\begin{pmatrix} i_1 \ldots i_p \\ k_1 \ldots k_p \end{pmatrix}. \tag{9}$$

Calculation of the $L-S-V$ coefficients with the use of (9) leads to the following expressions:

$$L = \sum_{i=1}^{n} \boldsymbol{\rho}_i \cdot \boldsymbol{f}_i, \tag{10}$$

$$S = \sum_{i=1}^{n} \sum_{j=i+1}^{n} (\boldsymbol{\rho}_i \times \boldsymbol{\rho}_j) \cdot (\boldsymbol{f}_i \times \boldsymbol{f}_j), \tag{11}$$

$$V = \sum_{i=1}^{n} \sum_{j=i+1}^{n} \sum_{k=j+1}^{n} \{\boldsymbol{\rho}_i \cdot (\boldsymbol{\rho}_j \times \boldsymbol{\rho}_k)\}\{\mathbf{f}_i \cdot (\mathbf{f}_j \times \boldsymbol{f}_k)\}. \tag{12}$$

Here, in order to highlight the geometric meaning of the $L-S-V$ coefficients, dots are used to designate the scalar product of two vectors.

Note that $\boldsymbol{K}$ is symmetric since the object is at equilibrium. By the Jacobi criterion,[20] a symmetric matrix is positive definite iff its characteristic polynom has sign-changing coefficients. Rewrite (8) as

$$\lambda^3 - 2L\lambda^2 + (L^2 + S)\lambda - (LS - V) = 0, \tag{13}$$

and the following stability conditions

$$L \ge 0, \tag{14}$$

$$L^2 + S \ge 0, \tag{15}$$

$$LS - V \ge 0, \tag{16}$$

are obtained for the matrix $\boldsymbol{K}$. The condition (14) has the following interpretation: the total work of the contact forces on the displacements defined by the contact point vectors must not be negative.

Note that if $\boldsymbol{K}$ is not symmetric, i.e. the object is not at equilibrium, the more general Routh-Hurwicz criterion should be used to judge on the positive definiteness of $\boldsymbol{K}$. As can be shown, one more stability condition* will be added to the set (14–16) in this case. This additional condition is not considered here, since the analysis of the asymmetric matrix $\boldsymbol{K}$ is out of the scope of this paper.

The $L-S-V$ coefficients are convenient for analysis of stability since they do not depend on the choice of the object reference frame. The coefficients are expressed in terms of the scalar, vector, and triple scalar products. Furthermore, they are symmetric with respect to the contact points and the contact forces, and some simple conclusions may be formulated straight away.

- The object is planar (the contact point vectors lie in a plane) or the contact forces are in a plane. In these cases $V = 0$ and the remaining stability conditions are

  $$L \ge 0 \text{ and } S \ge 0. \tag{17}$$

  It follows from (8) that the eigenvalues of $\boldsymbol{K}$, which can be thought of as rotational stiffnesses about the directions given by the eigenvectors of $\boldsymbol{K}$, are defined as follows in this case:

  $$\lambda_1 = L, \quad \lambda_{2,3} = \frac{L \pm \sqrt{L^2 - 4S}}{2}. \tag{18}$$

  Note also that if the object is planar the out-of-plane force components do not influence L and S.
- The object is one-dimensional (the contact point vectors lie on a line) or the system of contact forces is parallel. In these cases $V = 0$ and $S = 0$, and the remaining stability condition is $L \ge 0$.
- The object is planar and the contact forces lie in the orthogonal plane. In this case $V = 0$, $S = 0$ and $L = 0$, and the contact forces do not contribute to the stiffness tensor $\boldsymbol{K} = \boldsymbol{0}$.

More specific conclusions on the stability depend on the specific contact point and contact force distribution. However, in some situations it is possible to judge on the stability without long calculations. For example, one can prove that any force distribution in a frictionless grasp of a convex body is always unstable, since the angle between the normal contact force and the corresponding contact point vector is always more than $\pi/2$ and therefore $L < 0$.

4. STABILITY ANALYSIS

To establish relationships between the stability and the force structure, a proper decomposition of the applied forces is necessary. One possible decomposition is based on the pseudo-inversion[21] of the grasp matrix. Such a decomposition, interpreted in terms of the screw theory, has been developed[22] and its correctness has been shown.[23]

Under the pseudo-inverse decomposition, the applied forces $\boldsymbol{f}$ are separated orthogonally into the gravity forces and the internal forces. Similarly, the stiffness tensor $\boldsymbol{K}$ can be decomposed into the gravity-inducing component and the internal-force-inducing component. In what follows, the conditions under which the corresponding stiffness matrices become positive semi-definite, are established.

* The additional condition is $2L(L^2 + S) \ge LS - V$.

https://doi.org/10.1017/S0263574799002465 Published online by Cambridge University Press

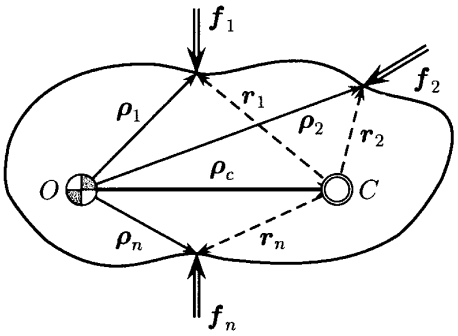

Fig. 1. Shift to the geometric center.

4.1. Gravity-induced stiffness

Consider stability due to the gravity force, assuming there is no internal force loading. To facilitate the calculations, the reference point O is shifted to the geometric center C (Figure 1) defined by

$$\boldsymbol{\rho}_c = \frac{1}{n}\sum_{i=1}^{n}\boldsymbol{\rho}_i. \tag{19}$$

Introducing the block vectors $\boldsymbol{\Phi}_0 = \{-m\boldsymbol{g} \equiv \boldsymbol{f}_c,\ \mathbf{0}\}^{\mathrm{T}}$ and $\boldsymbol{f} = \{\boldsymbol{f}_1^{\mathrm{T}}, \ldots, \boldsymbol{f}_n^{\mathrm{T}}\}^{\mathrm{T}}$, write down the static equations in the following form:

$$\boldsymbol{\Phi}_o = \boldsymbol{B}_o\boldsymbol{f} = \boldsymbol{B}_{oc}\boldsymbol{B}_c\boldsymbol{f}, \tag{20}$$

where

$$\boldsymbol{B}_{oc} = \begin{bmatrix} \boldsymbol{I} & \boldsymbol{O} \\ \boldsymbol{\Omega}(\boldsymbol{\rho}_c) & \boldsymbol{I} \end{bmatrix}, \quad \boldsymbol{B}_c = \begin{bmatrix} \boldsymbol{I} & \ldots & \boldsymbol{I} \\ \boldsymbol{\Omega}(\boldsymbol{r}_1) & \ldots & \boldsymbol{\Omega}(\boldsymbol{r}_n) \end{bmatrix}, \tag{21}$$

and $\boldsymbol{r}_i = \boldsymbol{\rho}_i - \boldsymbol{\rho}_c$. If $n \geq 3$ ($n \geq 2$ in the planar case) and the contact points do not lie on a common line, $\boldsymbol{B}_{oc}\boldsymbol{B}_c$ is a full-rank decomposition of the grasp matrix $\boldsymbol{B}_o$ and, therefore, $\boldsymbol{B}_o^{+} = \boldsymbol{B}_c^{+}\boldsymbol{B}_{oc}^{-1}$.

The pseudo-inverse solution of (20) is given by

$$\boldsymbol{f} = \boldsymbol{B}_o^{+}\boldsymbol{\Phi}_o = \boldsymbol{B}_c^{\mathrm{T}}(\boldsymbol{B}_c\boldsymbol{B}_c^{\mathrm{T}})^{-1}\boldsymbol{B}_{oc}^{-1}\boldsymbol{\Phi}_o,$$

where the matrix $\boldsymbol{B}_c\boldsymbol{B}_c^{\mathrm{T}}$ is block-diagonal, $\boldsymbol{B}_c\boldsymbol{B}_c^{\mathrm{T}} = \mathrm{diag}\{n\boldsymbol{I}, \boldsymbol{J}_c\}$, because $\sum_{i=1}^{n}\boldsymbol{r}_i = \mathbf{0}$. Computing (22) in the block-component form, one obtains the following representation for the gravity-induced forces

$$\boldsymbol{f}_i = \frac{1}{n}\boldsymbol{f}_c + \boldsymbol{r}_i \times \boldsymbol{J}_c^{-1}(\boldsymbol{\rho}_c \times \boldsymbol{f}_c), \quad i = 1, \ldots, n, \tag{23}$$

where

$$\boldsymbol{J}_c = \sum_{i=1}^{n}(\boldsymbol{r}_i^{\mathrm{T}}\boldsymbol{r}_i)\boldsymbol{I} - \boldsymbol{r}_i\boldsymbol{r}_i^{\mathrm{T}} \tag{24}$$

is the contact point tensor. It is the inertia tensor of a system formed by the unit mass points $\boldsymbol{r}_i$. In the general spatial case $\boldsymbol{J}_c \in \Re^{3\times 3}$ is symmetric and positive definite if $n \geq 3$ and all points do not lie on a common line.

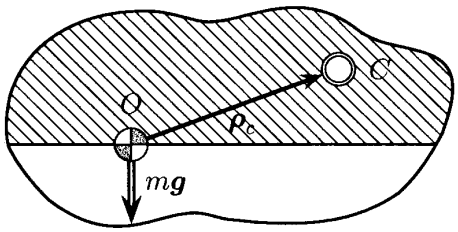

Fig. 2. Gravitational stability as given by $L > 0$.

The gravity-induced stiffness tensor and the corresponding $L-S-V$ coefficients can be represented through the geometric parameters of the grasp, $\boldsymbol{\rho}_c$ and $\boldsymbol{J}_c$. Substituting (23) into (10–12) leads to the following expressions:

$$L = \boldsymbol{\rho}_c^{T}\boldsymbol{f}_c, \tag{25}$$

$$S = (\boldsymbol{\rho}_c \times \mathbf{J}_c\boldsymbol{f}_c)^{\mathrm{T}}\boldsymbol{J}_c^{-1}\boldsymbol{m}_c + \boldsymbol{m}_c^{\mathrm{T}}(\boldsymbol{I} - 2l\boldsymbol{J}_c^{-1} + s\boldsymbol{J}_c^{-2})\boldsymbol{m}_c, \tag{26}$$

$$V = \{\boldsymbol{\rho}_c^{\mathrm{T}}(\boldsymbol{J}_c + s\boldsymbol{J}_c^{-1})\boldsymbol{m}_c\}\ \ \{\boldsymbol{f}_c^{\mathrm{T}}\boldsymbol{J}_c^{-1}\boldsymbol{m}_c\}, \tag{27}$$

where $\boldsymbol{m}_c = \boldsymbol{\rho}_c \times \boldsymbol{f}_c$ is the gravitational moment, and l, s, υ are the $L-S-V$ coefficients for the contact point tensor $\boldsymbol{J}_c$.

Note that the stability condition (14) has now the following geometric interpretation: for the no-internal-force grasp to be stable, the geometric center $\boldsymbol{\rho}_c$ must be placed above the center of mass of the object. (Figure 2).

In general, the gravitational stability depends on $\boldsymbol{f}_c$, $\boldsymbol{\rho}_c$, and $\boldsymbol{J}_c$. Some particular cases, when the stability judgement can be done easily, are listed below.

Case 1. *If the geometric center of the grasp coincides with the center of mass* ($\boldsymbol{\rho}_c = \mathbf{0}$), *gravity does not contribute to the total stiffness.*

Case 2. *The vectors* $\boldsymbol{\rho}_c$ *and* $\boldsymbol{f}_c$ are parallel, i.e., $\boldsymbol{f}_c = k\boldsymbol{\rho}_c$ and $\boldsymbol{m}_c = 0$. *In this case* $V = 0$, $S = 0$ *and the remaining stability condition* $L \geq 0$ *gives* $k \geq 0$.

Note that if a configuration is stable for $\boldsymbol{f}_c = \boldsymbol{f}_c^{*}$, it will also be stable for $\boldsymbol{f}_c = \boldsymbol{f}_c^{*} + k\boldsymbol{\rho}_c$.

Case 3. *If* $\boldsymbol{f}_c$ *is parallel to one of the eigen-vectors of* $\boldsymbol{J}_c$, *or* $\boldsymbol{\rho}_c$ *is parallel to one of the eigen-vectors of* $\boldsymbol{J}_c$, *then* $V = 0$ *and* S *is always negative unless* $\boldsymbol{m}_c = 0$.

To prove it, consider all the vector quantities in the principal axes of the tensor $\boldsymbol{J}_c$. In the principal axes, $\boldsymbol{J}_c^{(c)} = \mathrm{diag}\{J_x, J_y, J_z\}$.

First, consider the case of $\boldsymbol{J}_c\boldsymbol{f}_c = \lambda\boldsymbol{f}_c$. Let $\boldsymbol{\rho}_c^{(c)} = \{\rho_x,\ \rho_y,\ \rho_z\}^{\mathrm{T}}$, and also let $\boldsymbol{f}_c$ be parallel, for example, to the x eigen-direction of $\boldsymbol{J}_c$, i.e., $\boldsymbol{f}_c^{(c)} = \{f_x,\ 0,\ 0\}^{\mathrm{T}}$. Then, calculation by (26) gives

$$S = -\frac{f_x^2(-J_x + J_y + J_z)^2\,(J_y^2\rho_y^2 + J_z^2\rho_z^2)}{4\,J_y^2\,J_z^2}. \tag{28}$$

By the triangle inequality for moments of inertia $J_y + J_z > J_x$, and $S = 0$ only if $\rho_y = 0$ and $\rho_z = 0$, i.e. $\boldsymbol{m}_c = 0$.

Next, consider the case of $\boldsymbol{J}_c\boldsymbol{\rho}_c = \lambda\boldsymbol{\rho}_c$. Let $\boldsymbol{f}_c^{(c)} = \{f_x, f_y, f_z\}^{\mathrm{T}}$ and also let $\boldsymbol{\rho}_c$ be parallel to the x eigen-direction of $\boldsymbol{J}_c$, i.e., $\boldsymbol{\rho}_c^{(c)} = \{\rho_x, 0, 0\}^{\mathrm{T}}$. Then,

$$S = -\frac{\rho_x^2\{(J_x + J_y - J_z)^2J_z^2f_z^2 + (J_x + J_z - J_y)^2J_y^2f_y^2\}}{4J_y^2J_z^2}. \tag{29}$$

Again, taking into account the triangle inequalities, one concludes that $S = 0$ only if $f_y = 0$ and $f_z = 0$, i.e. $\boldsymbol{m}_c = 0$.

https://doi.org/10.1017/S0263574799002465 Published online by Cambridge University Press

Case 3 covers the case when the contact points form a regular polyhedron configuration (tetrahedron, cube, octahedron, dodecahedron, icosahedron). For the regular polyhedrons, $\boldsymbol{J}_c$ is proportional to the unit tensor, and $\boldsymbol{f}_c$ is always on one of the eigen-directions of $\boldsymbol{J}_c$. Another particular case, covered by Case 3, is when the object is planar and its plane is orthogonal to the gravity force. Note that in the latter case $L = 0$, and $\boldsymbol{m}_c = 0$ means $\boldsymbol{\rho}_c = 0$.

Case 4. *The vector $\boldsymbol{m}_c$ is parallel to one of the eigen-vectors of $\boldsymbol{J}_c$. In this case $V = 0$ because $\boldsymbol{J}_c\boldsymbol{m}_c = \lambda\boldsymbol{m}_c$, and the vectors $\boldsymbol{f}_c$ and $\boldsymbol{\rho}_c$ lie in a plane orthogonal to one of the eigen-vectors of $\boldsymbol{J}_c$.*

Without loss of generality, put $\boldsymbol{f}_c^{(c)} = \{f_x, f_y, 0\}^{\mathrm{T}}$ and $\boldsymbol{\rho}_c^{(c)} = \{\boldsymbol{\rho}_x, \boldsymbol{\rho}_y, 0\}^{\mathrm{T}}$, and transform $\boldsymbol{f}_c$ and $\boldsymbol{\rho}_c$ to the polar coordinates: $f_x = f\sin\varphi$, $f_y = f\cos\varphi$, $\rho_x = \rho\sin\psi$, $\rho_y = \rho\cos\psi$. Calculation by (25) gives $L = f\rho\cos(\varphi - \psi)$ and the area of $L > 0$ is defined as $-\pi/2 < \varphi - \psi < \pi/2$.

Next, formula (26) gives

$$S = -\frac{f^2\rho^2\sin(\varphi-\psi)\{\sin\varphi\cos\psi - z^2\cos\vartheta\sin c\}}{1+z^2}, \quad (30)$$

where

$$z = \frac{J_z - J_x + J_y}{J_z + J_x - J_y}. \quad (31)$$

As can be seen from (30), $S = 0$ when $\varphi - \psi = \pm k\pi$ or $\tan\varphi\tan^{-1}\psi = z^2$. Sign of S does not depend on the absolute values of $\boldsymbol{\rho}_c$ and $\boldsymbol{f}_c$. Areas of $S \geq 0$ are shown in gray color in Figure 3 for $z = 2$ (top) and $z = 10$ (bottom). As $z \to 1$ the areas transform to lines $\varphi - \psi = \pm k\pi$, and reflect symmetrically when $z < 1$. Note, finally, that Case 4 covers the case when all the contact points and the gravity force lie in a plane. Here, $J_z = J_x + J_y$ and $z = J_y/J_x$.

4.2. Internal-force-induced stiffness

Consider now stability due to the internal forces. The general solution of the static equations (20) for $\boldsymbol{\Phi}_o = \boldsymbol{0}$ has the following form:

$$\boldsymbol{f} = \boldsymbol{P}_c\boldsymbol{\varphi} = (I - \boldsymbol{B}_c^{+}\boldsymbol{B}_c)\boldsymbol{\varphi}, \quad (32)$$

where $\boldsymbol{P}_c$ is the orthogonal projector onto the null space of the grasp matrix $\boldsymbol{B}_o$, i.e., onto the space of the internal forces, and $\boldsymbol{\varphi} \in \mathbb{R}^{3n}$ is an arbitrary vector.

Note that $\boldsymbol{\varphi}$ defines a redundant representation of the internal forces and does not have a clear physical meaning. To introduce a physically meaningful parameterization of the internal forces, one can characterize the interaction between any two fingers by[22]

$$\alpha_{ij} = (\boldsymbol{r}_i - \boldsymbol{r}_j)^{\mathrm{T}}(\boldsymbol{f}_i - \boldsymbol{f}_j). \quad (33)$$

i.e., by the difference of the contact forces projected along the line joining the two contact points. The interaction force is of compression type if $\alpha_{ij} < 0$, and of tension type if $\alpha_{ij} > 0$.

The physical meaning of α_{ij} is the work produced by $\boldsymbol{f}_{ij} = \boldsymbol{f}_i - \boldsymbol{f}_j$ on the displacement $\boldsymbol{r}_{ij} = \boldsymbol{f}_i - \boldsymbol{f}_j$. However, the dimension of α_{ij}, [N · m], can also be interpreted as that of the rotational stiffness. It is remarkable that in this interpretation the grasp of a rigid body can be represented by virtual springs which can have positive as well as negative stiffness.

Summing up all α_{ij} as given by (33) and comparing the result with (10) gives

$$L = \frac{1}{n}\sum_{i=1}^{n}\sum_{j=i+1}^{n}\alpha_{ij}, \quad (34)$$

The stability condition (14) has now the following interpretation: the total stiffness of the rotational virtual springs must not be negative.

Equations (33) can be represented in the matrix form

$$\boldsymbol{\alpha} = \boldsymbol{A}_o\boldsymbol{f}, \quad (35)$$

where $\boldsymbol{\alpha} = \{\alpha_{ij}\} \in \mathbb{R}^N$, $N = n(n-1)/2$, and $\boldsymbol{A}_o \in \mathbb{R}^{N\times 3n}$. This representation depends on how the elements of $\boldsymbol{\alpha}$ are ordered. For example, for the three-fingered grasp (Figure 4) with $\boldsymbol{\alpha} = \{\alpha_{23}, \alpha_{31}, \alpha_{12}\}^{\mathrm{T}}$, the matrix $\boldsymbol{A}_o$ can be constructed as follows:

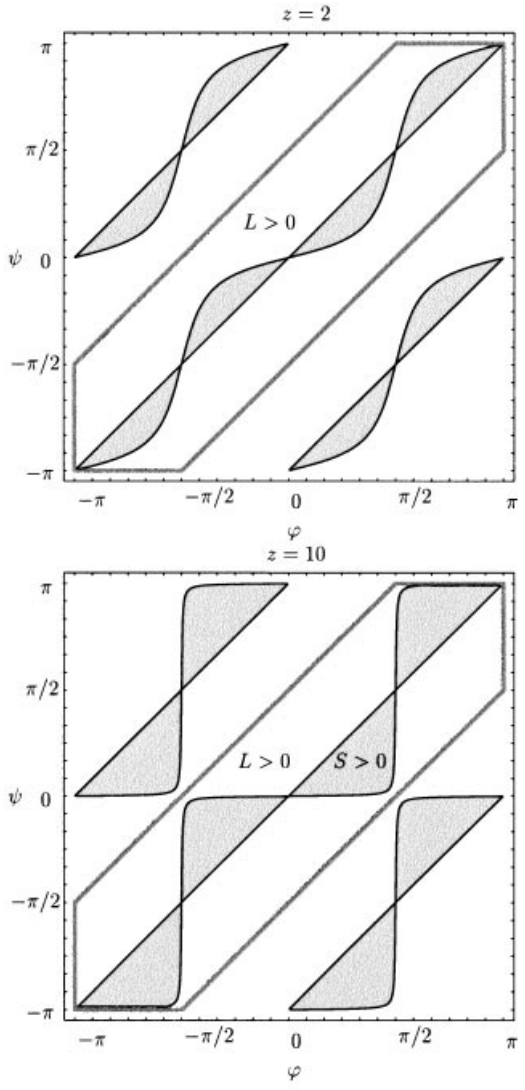

Fig. 3. Areas of positive S.

https://doi.org/10.1017/S0263574799002465 Published online by Cambridge University Press

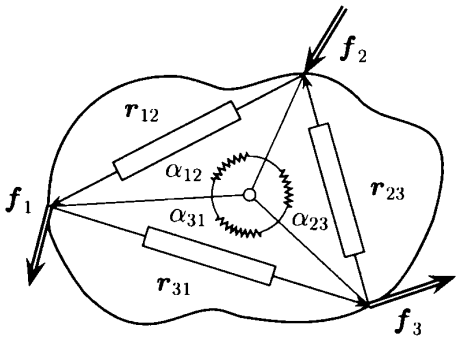

Fig. 4. Rotational springs in three-fingered grasp.

$$\boldsymbol{A}_o = \begin{bmatrix} \mathbf{0} & \boldsymbol{r}_{23}^{\mathrm{T}} & -\boldsymbol{r}_{23}^{\mathrm{T}} \\ -\boldsymbol{r}_{31}^{\mathrm{T}} & \mathbf{0} & \boldsymbol{r}_{31}^{\mathrm{T}} \\ \boldsymbol{r}_{12}^{\mathrm{T}} & -\boldsymbol{r}_{12}^{\mathrm{T}} & \mathbf{0} \end{bmatrix}. \tag{36}$$

For the minimal, non-redundant representation of the internal forces—for which there exists a one-to-one mapping between the internal forces $\boldsymbol{f}$ and the vector $\boldsymbol{\alpha}$—the dimension of $\boldsymbol{\alpha}$ should be equal to the dimension of the null space of the grasp matrix $\boldsymbol{B}_o$. Equating N to $3(n-2)$ gives $n=3$ or $n=4$.

Note that for an arbitrary $\boldsymbol{\beta} = \{\beta_{ij}\} \in \mathbb{R}^N$ the vector

$$\boldsymbol{f} = \boldsymbol{A}_o^T \boldsymbol{\beta} \tag{37}$$

belongs to the null space of the grasp matrix $\boldsymbol{B}_o$. Here, parameterization of the internal forces is done in terms of the linear virtual springs (Figure 5), with β_{ij} being the stiffness of the spring connecting the i-th and j-th contact points. It should be noted that this interpretation is conceptually close to the virtual linkage model[24] and to the virtual truss model.[25]

Combining (35) with (37) gives the following relationship between stiffness of the linear and the rotational virtual springs:

$$\boldsymbol{\beta} = (\boldsymbol{A}_o \boldsymbol{A}_o^{\mathrm{T}})^{-1} \boldsymbol{\alpha}. \tag{38}$$

The transformation from the rotational to the linear virtual springs is nonsingular if the grasp is non-degenerative and $n \le 7$.

Now, assume that the elements β_{ij} of the vector $\boldsymbol{\beta}$ are somehow ordered, and can be addressed by only one subscript. The same order is kept for the corresponding vectors $\boldsymbol{r}_{ij}$ and $\boldsymbol{f}_{ij}$. The use of such single-indexed variables is marked by bar sign, i.e., $\bar{\beta}_l$ corresponds to some element β_{ij}.

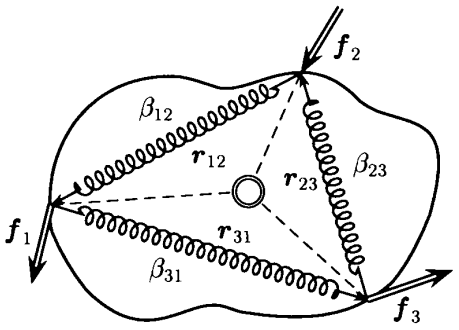

Fig. 5. Linear springs in three-fingered grasp.

In synthesis of a stable grasp under the internal force loading the stiffness of the linear virtual springs should be specified in such a way so that the stiffness tensor is positive semi-definite. Substituting the internal forces (37) into (3) gives

$$\boldsymbol{K} = \sum_{i=1}^{N} \bar{\beta}_i \{ (\bar{\boldsymbol{r}}_i^{\mathrm{T}} \bar{\boldsymbol{r}}_i) \boldsymbol{I} - \bar{\boldsymbol{r}}_i \bar{\boldsymbol{r}}_i^{\mathrm{T}} \}. \tag{39}$$

As can be seen, $\boldsymbol{K}$ has the structure of the inertia tensor of a system of points built on the vectors $\bar{\boldsymbol{r}}_i$, with $\bar{\beta}_i$ playing the role of masses. Hence, N conditions $\beta_i \ge 0$ guarantee that the matrix $\boldsymbol{K}$ is not negative definite. However, they are the sufficient but not necessary conditions for stability under the internal forces.

The necessary and sufficient conditions are given by (14–16) where the $L-S-V$ coefficients are defined as follows:

$$L = \sum_{i=1}^{N} \bar{\beta}_i \, (\bar{\boldsymbol{r}}_i \cdot \bar{\boldsymbol{r}}_i), \tag{40}$$

$$S = \sum_{i=1}^{N} \sum_{j=i+1}^{N} \bar{\beta}_i \bar{\beta}_j (\bar{\boldsymbol{r}}_i \times \bar{\boldsymbol{r}}_j) \cdot (\bar{\boldsymbol{r}}_i \times \bar{\boldsymbol{r}}_j), \tag{41}$$

$$V = \sum_{i=1}^{N} \sum_{j=i+1}^{N} \sum_{k=j+1}^{N} \bar{\beta}_i \bar{\beta}_j \bar{\beta}_k \{ \bar{\boldsymbol{r}}_i \cdot (\bar{\boldsymbol{r}}_j \times \bar{\boldsymbol{r}}_k) \}^2, \tag{42}$$

They are obtained from (10–12) with the formal change: $\boldsymbol{\rho}_i \to \bar{\boldsymbol{r}}_i$ and $\boldsymbol{f}_i \to \bar{\beta}_i \bar{\boldsymbol{r}}_i$.

Consider, for a example, a three-fingered grasp. In this case the vectors $\bar{\mathbf{r}}_i$, $\bar{\mathbf{r}}_j$, $\bar{\mathbf{r}}_k$ are linearly dependent, and therefore $V=0$. The remaining stability conditions are $L \ge 0$ and $S \ge 0$. One can show that

$$S = \boldsymbol{n}^{\mathrm{T}} \boldsymbol{n} (\bar{\beta}_1 \bar{\beta}_2 + \bar{\beta}_2 \bar{\beta}_3 + \bar{\beta}_3 \bar{\beta}_1), \tag{43}$$

where the vector

$$\boldsymbol{n} = \boldsymbol{r}_1 \times \boldsymbol{r}_2 + \boldsymbol{r}_2 \times \boldsymbol{r}_3 + \boldsymbol{r}_3 \times \boldsymbol{r}_1 \tag{44}$$

is orthogonal to the plane containing the contact points. If the grasp is non-degenerative $\boldsymbol{n} \ne \mathbf{0}$, and $S \ge 0$ is equivalent to

$$\bar{\beta}_1 \bar{\beta}_2 + \bar{\beta}_2 \bar{\beta}_3 + \bar{\beta}_3 \bar{\beta}_1 \ge 0. \tag{45}$$

Geometrically, the stability area in the space $\bar{\beta}_1$, $\bar{\beta}_2$, $\bar{\beta}_3$ is defined by the intersection of the plane $L>0$ with the cone (45).

5. FRICTIONAL CONSTRAINTS

For systems with bilateral constraints between the object and the end-point links, the conditions (14–16) can be achieved more or less easily provided there is enough power. In grasping, however, the constraints are unilateral. Commonly, they are defined on the basis of the Coulomb friction models:

https://doi.org/10.1017/S0263574799002465 Published online by Cambridge University Press

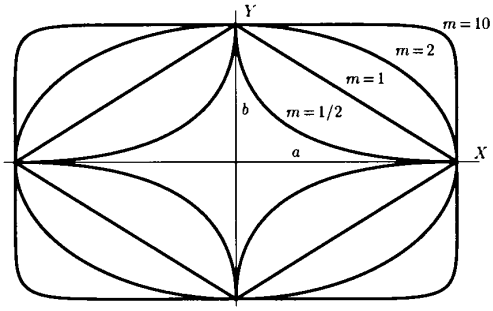

Fig. 6. Object shapes.

$$|\, \boldsymbol{n}_i \times \boldsymbol{f}_i \,| \le \mu (\boldsymbol{f}_i \cdot \boldsymbol{n}_i),\ i = 1, \ldots, n, \tag{46}$$

where $\boldsymbol{n}_i$ is the unit vector orthogonal to the object's surface, pointing toward it, and μ stands for the static friction coefficient.

In this section, we study the conditions (14–16) under the constraints (46) for a simple example. Consider a planar object, grasped by a four-fingered hand. The geometric form of the object is that of the generalized ellipse:

$$\left(\frac{x}{a}\right)^m + \left(\frac{y}{b}\right)^m = 1, \tag{47}$$

where a and b are the lengths of the semi-axes of the ellipse. The object is convex for $m \ge 1$, and concave for $m < 1$ (see Figure 6).

Assume the symmetrical placement of the contact points on the object as shown in Figure 7 for $m = 2$. The contact points are defined as follows:

$$\boldsymbol{\rho}_1 = \begin{bmatrix} \alpha \cos^{2/m}\psi \\ b \sin^{2/m}\psi \\ 0 \end{bmatrix},\ \boldsymbol{\rho}_2 = \begin{bmatrix} -\alpha \cos^{2/m}\psi \\ b \sin^{2/m}\psi \\ 0 \end{bmatrix}, \tag{48}$$

and $\boldsymbol{\rho}_3 = -\boldsymbol{\rho}_1$, $\boldsymbol{\rho}_4 = -\boldsymbol{\rho}_2$. Here, $\psi \in [0, \pi/2]$ is the grasping angle.

The inward normals to the surface at the contact points are defined as follows:

$$\boldsymbol{n}_1 = \begin{bmatrix} \dfrac{-b \sin^{\frac{2}{m}}\psi \cos^2\psi}{\lambda(\psi)} \\ \dfrac{-a \cos^{\frac{2}{m}}\psi \sin^2\psi}{\lambda(\psi)} \\ 0 \end{bmatrix},\ \boldsymbol{n}_2 = \begin{bmatrix} \dfrac{b \sin^{\frac{2}{m}}\psi \cos^2\psi}{\lambda(\psi)} \\ \dfrac{-a \cos^{\frac{2}{m}}\psi \sin^2\psi}{\lambda(\psi)} \\ 0 \end{bmatrix}, \tag{49}$$

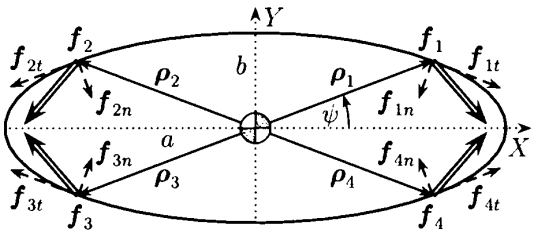

Fig. 7. Four-fingered grasp.

$\boldsymbol{n}_3 = -\boldsymbol{n}_1$, $\boldsymbol{n}_4 = -\boldsymbol{n}_2$, where

$$\lambda(\psi) = \sqrt{a^2 \cos^{4/m}\psi \sin^4\psi + b^2 \sin^{4/m}\psi \cos^4\psi}. \tag{50}$$

To specify the positive directions of the friction forces, define the clockwise (at the 1st and 3rd points) and counter-clockwise (at the 2nd 4th points) tangential vectors:

$$\boldsymbol{\tau}_1 = \begin{bmatrix} \dfrac{a \cos^{\frac{2}{m}}\psi \sin^2\psi}{\lambda(\psi)} \\ \dfrac{-b \sin^{\frac{2}{m}}\psi \cos^2\psi}{\lambda(\psi)} \\ 0 \end{bmatrix},\ \boldsymbol{\tau}_2 = \begin{bmatrix} \dfrac{-a \cos^{\frac{2}{m}}\psi \sin^2\psi}{\lambda(\psi)} \\ \dfrac{-b \sin^{\frac{2}{m}}\psi \cos^2\psi}{\lambda(\psi)} \\ 0 \end{bmatrix}, \tag{51}$$

and $\boldsymbol{\tau}_3 = -\boldsymbol{\tau}_1$, $\boldsymbol{\tau}_4 = -\boldsymbol{\tau}_2$.

Consider the force distribution given by

$$\boldsymbol{f}_i = f_n\ \boldsymbol{n}_i + f_t \boldsymbol{\tau}_i,\ i = 1,\ \ldots,\ 4. \tag{52}$$

No gravity is assumed, the static equations are always satisfied under the specified contact forces. The object is stretched in the X direction if $f_t > 0$ and compressed if $f_t < 0$. The unilateral constraints on the normal forces are given by $f_n \ge 0$, and the Coulomb friction constraints (46) take the following form:

$$-\mu \le f_t / f_n \le \mu. \tag{53}$$

The coefficient L, which has the meaning of the rotational stiffness of the object in the plane OXY, is calculated by (10). It is obtained as

$$L = \frac{4}{\lambda(\psi)} (f_t (a^2 \cos^{\frac{4}{m}}\psi \sin^2\psi - b^2 \sin^{\frac{4}{m}}\psi \cos^2\psi) - f_n\, ab \cos^{\frac{2}{m}}\psi \sin^{\frac{2}{m}}\psi). \tag{54}$$

Note that the rotational stiffness is not positive if $f_t = 0$ (for example, if there is no friction). Also, there exists* a critical value of the grasping angle, defined from

$$\tan^{-1+2/m}\psi = a/b, \tag{55}$$

under which L becomes negative because it does not depend on f_t. The geometric meaning of the condition (55) is that $\boldsymbol{\rho}_i$ is orthogonal to $\boldsymbol{\tau}_i$ under (55). Also, it can be shown that for $a = b$ the curvature of the object attains its extremal value for the grasping angle given by (55).

From the condition $L > 0$ one gets

$$\frac{f_t}{f_n} \ge \pm \frac{ab \cos^{2/m}\psi \sin^{2/m}\psi}{a^2 \cos^{4/m}\psi \sin^2\psi - b^2 \sin^{4/m}\psi \cos^2\psi}, \tag{56}$$

where plus is taken if $a/b > \tan^{-1+2/m}\psi$, and minus otherwise. The force distribution (52) is both admissible and stable if there is a solution for the system of inequalities (53, 56).

Dependence on the parameter *m*. Put $a = b$ and change the parameter m. The plots, corresponding to three possible

* *Except of* $m = 2$ and $a \ne b$.

https://doi.org/10.1017/S0263574799002465 Published online by Cambridge University Press

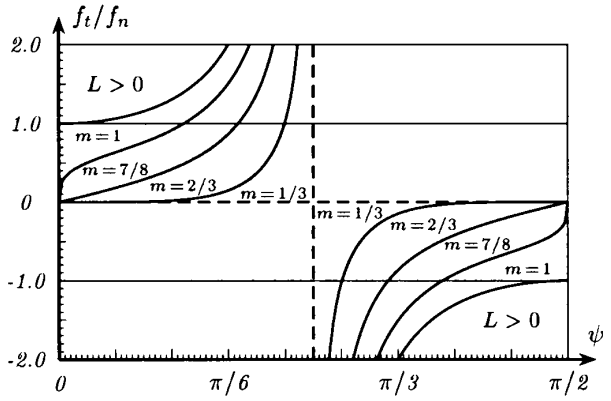

Fig. 8. Concave shape of the object ($m < 1$).

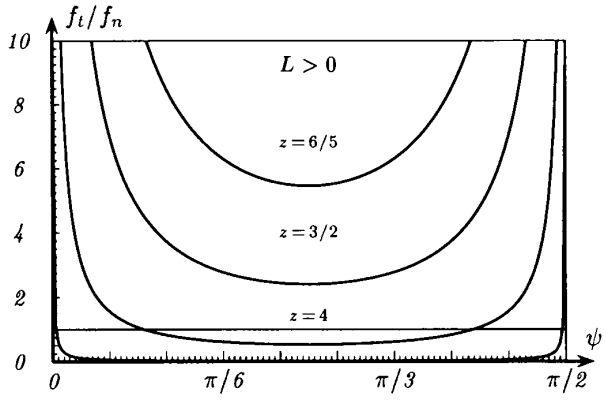

Fig. 11. Convex shape of the object ($m = 2$, $a > b$).

situations, $m < 1$, $1 < m < 2$, and $m > 2$, are shown in Figures 8, 9 and 10.

As can be seen from Figure 8, for the concave shapes there always exist grasping angles for which (56) has intersection with the area of "realistic" friction coefficients $|f_t/f_n| \le 1$. However, as m tends to 1, the solution area gets smaller and finally converges to two points (0 for $f_t > 0$, and $\pi/2$ for $f_t < 0$). But what is more important is that for any μ there exist grasping angles ψ for which the force distribution (52) is stable.

As to the convex shapes, (56) has no intersection with the area of "realistic" friction coefficients $|f_t/f_n| \le 1$. Thus, a higher friction coefficient is required to achieve stable force distribution of the convex object. Finally, note that the case $m = 2$ (sphere) is singular in the sense that L does not depend on f_t and is always negative. Therefore, the force distribution is always unstable for the case of sphere.

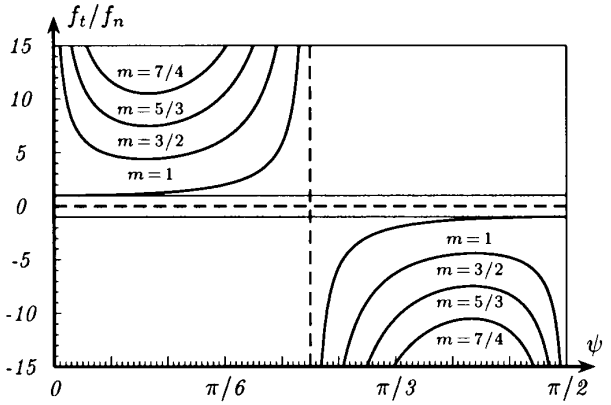

Fig. 9. Convex shape of the object ($1 < m < 2$).

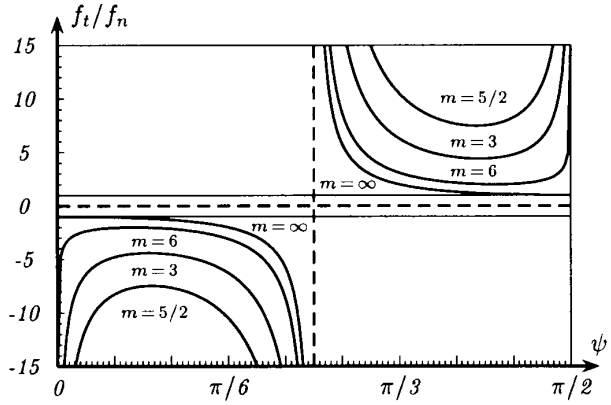

Fig. 10. Convex shape of the object ($m < 2$).

Dependence on the ratio *a/b*. Put $m = 2$ (singular case in the previous model) and change the ratio $z = a/b$. Without loss of generality, assume $a > b$, i.e. $z > 1$. Inequality (56) is simplified and takes the following form (Figure 11):

$$\frac{f_t}{f_n} \ge \frac{z}{z^2 - 1} \frac{2}{\sin 2\psi}. \tag{57}$$

As can be easily seen, the line of zero L in the plane f_t/f_n, ψ attains its minimum, $2z/(z^2 - 1)$, at $\psi = \pi/4$. The minimum goes to infinity as $z \to 1$ (sphere). For the force distribution (52) to be both admissible and stable, one must require $2z/(z^2 - 1) < \mu$, which leads to the following estimate:

$$z > \frac{1 + \sqrt{1 + \mu^2}}{\mu}. \tag{58}$$

For example, for $\mu = 0.2$ it gives, roughly, $a > 10b$.

Spatial case. The pure planar case was analyzed so far. Now, assume that the grasping takes place in the three-dimensional space.* The coefficient S is calculated by (11) and is defined as

$$S = -\frac{16ab \cos^{\frac{2}{m}}\psi \sin^{\frac{2}{m}}\psi}{\lambda^2(\psi)}$$
$$(f_n f_t (a^2 \cos^{\frac{4}{m}}\psi \sin^4\psi - b^2 \sin^{\frac{4}{m}}\psi \cos^4\psi)$$
$$+ (f_t^2 - f_n^2)ab \cos^{\frac{2m+2}{m}}\psi \sin^{\frac{2m+2}{m}}\psi). \tag{59}$$

The condition $S > 0$ takes the following form

$$-\frac{a}{b}\tan^{2-2/m}\psi \le \frac{f_t}{f_n} \le \frac{b}{a}\tan^{-2+2/m}\psi. \tag{60}$$

It can be shown that regardless of the friction coefficient μ the areas of $L > 0$ and $S > 0$ do not have intersection in the

* One can imagine a cylindrical object with the cross-section (grasping plane) having the form of the generalized ellipse.

https://doi.org/10.1017/S0263574799002465 Published online by Cambridge University Press

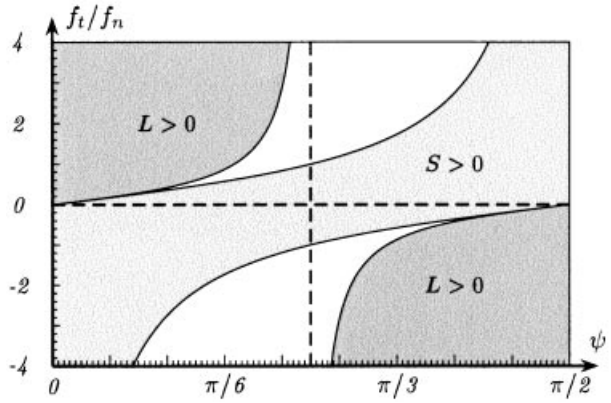

Fig. 12. Concave shape of the object ($m = 2/3$).

plane f_t/f_n, ψ. This is illustrated in Figure 12 for $a = b$ and $m = 2/3$ (astroid). Thus, in the spatial case the force distribution (52) is not stable.

6. GRASP STABILIZATION

As shown in the previous section, the conditions (14–16) are not always achievable under the unilateral grasping constraints. In such situations the feedback stabilization is necessary. In this section, we consider a simple control law of the following form:

$$\Delta \boldsymbol{f}_i = -k_{vi}\,\Delta \dot{\boldsymbol{x}}_i - k_{pi}\,\Delta \boldsymbol{x}_i\,, \quad i = 1,\ \ldots,\ n, \tag{61}$$

where $\Delta \boldsymbol{x}_i$ are changes in the desired contact positions. Mechanically, it corresponds to the introduction of virtual linear springs—with stiffness $k_{pi} > 0$ and damping $k_{vi} > 0$—at the contact points.

The fingers are controlled locally and direct measurement of the object position and orientation is not required. Taking into account that $\Delta \boldsymbol{x}_i = \Delta \boldsymbol{x} + \boldsymbol{\theta} \times \boldsymbol{\rho}_i$ and $\Delta \dot{\boldsymbol{x}}_i = \Delta \dot{\boldsymbol{x}} + \dot{\boldsymbol{\theta}} \times \boldsymbol{\rho}_i$, it can be shown that the projection of the combined vector $\{\Delta \boldsymbol{f}_1^{\mathrm{T}}, \ldots, \Delta \boldsymbol{f}_n^{T}\}$ onto the internal force space is always zero. Hence, the control law (61) does not influence the internal force distribution. The linearized dynamic equations (2) under the feedback (61) become

$$\begin{bmatrix} m\boldsymbol{I} & \boldsymbol{O} \\ \boldsymbol{O} & \boldsymbol{J} \end{bmatrix} \begin{bmatrix} \Delta \ddot{\boldsymbol{x}} \\ \ddot{\boldsymbol{\theta}} \end{bmatrix} + \tag{62}$$

$$\sum_{i=1}^{n} k_{vi} \begin{bmatrix} \boldsymbol{I} & \boldsymbol{\Omega}^{\mathrm{T}}(\boldsymbol{\rho}_i) \\ \boldsymbol{\Omega}(\boldsymbol{\rho}_i) & \boldsymbol{\Omega}^{\mathrm{T}}(\boldsymbol{\rho}_i)\boldsymbol{\Omega}(\boldsymbol{\rho}_i) \end{bmatrix} \begin{bmatrix} \Delta \dot{\boldsymbol{x}} \\ \dot{\boldsymbol{\theta}} \end{bmatrix} +$$

$$\left(\begin{bmatrix} \boldsymbol{O} & \boldsymbol{O} \\ \boldsymbol{O} & \boldsymbol{K} \end{bmatrix} \right.$$

$$\left. + \sum_{i=1}^{n} k_{pi} \begin{bmatrix} \boldsymbol{I} & \boldsymbol{\Omega}^{\mathrm{T}}(\boldsymbol{\rho}_i) \\ \boldsymbol{\Omega}(\boldsymbol{\rho}_i) & \Omega^{\mathrm{T}}(\boldsymbol{\rho}_i)\boldsymbol{\Omega}(\boldsymbol{\rho}_i) \end{bmatrix} \right) \begin{bmatrix} \Delta \boldsymbol{x} \\ \boldsymbol{\theta} \end{bmatrix} = \boldsymbol{0}.$$

The grasp under the feedback (61) is asymptotically stable if the damping and stiffness matrices in (62) are positive definite. The corresponding conditions are established with the use of Theorem 7.7.6.[26] The damping matrix is positive definite if the matrix

$$\sum_{i=1}^{n} k_{vi}\, \boldsymbol{\Omega}^{\mathrm{T}}(\boldsymbol{\rho}_i - \boldsymbol{\rho}_d)\, \boldsymbol{\Omega}(\boldsymbol{\rho}_i - \boldsymbol{\rho}_d) \tag{63}$$

is positive definite. Here,

$$\boldsymbol{\rho}_d = \frac{\sum_{i=1}^{n} k_{vi} \boldsymbol{\rho}_i}{\sum_{i=1}^{n} k_{vi}} \tag{64}$$

is the center of damping. The matrix (63) is the damping tensor calculated at the damping center. The damping tensor has the structure of the inertia tensor of a system of points of mass k_{vi} built on the vectors $\boldsymbol{\rho}_i - \boldsymbol{\rho}_d$. In the general spatial it is positive definite if $n \geq 3$ and all points do not lie on a common line.

As to the stiffness matrix, it is positive definite if the matrix

$$\boldsymbol{K} + \sum_{i=1}^{n} k_{pi} \boldsymbol{\Omega}^{\mathrm{T}}(\boldsymbol{\rho}_i - \boldsymbol{\rho}_s) \boldsymbol{\Omega}\,(\boldsymbol{\rho}_i - \boldsymbol{\rho}_s) \tag{65}$$

is positive definite. Here,

$$\boldsymbol{\rho}_s = \frac{\sum_{i=1}^{n} k_{pi} \boldsymbol{\rho}_i}{\sum_{i=1}^{n} k_{pi}} \tag{66}$$

is the center of stiffness. The second part of (65) is the stiffness tensor of the "control" springs calculated at the stiffness center. This tensor has the structure of the inertia tensor of a system of points of mass k_{pi} built on the vectors $\boldsymbol{\rho}_i - \boldsymbol{\rho}_s$. Therefore, it is positive definite if $n > 3$ and all points do not lie on a common line.

It is concluded from (65) that the grasp is stable for any $k_{pi} > 0$ if the force distribution is stable. If, however, it is not the case and $\boldsymbol{K}$ is negative definite, one can always adjust k_{pi} so that to make (65) positive definite. To establish the stability conditions, transform the matrix (65) to the following form

$$\sum_{i=1}^{n} \boldsymbol{\Omega}^{\mathrm{T}} \{ \boldsymbol{f}_i + k_{pi}(\boldsymbol{\rho}_i - \boldsymbol{\rho}_s) \}\, \boldsymbol{\Omega}\,(\boldsymbol{\rho}_i). \tag{67}$$

One can see that the structure of the matrix (67) copies that of $\boldsymbol{K}$ with the formal change:

$$\boldsymbol{f}_i \rightarrow \boldsymbol{f}_i + k_{pi}(\boldsymbol{\rho}_i - \boldsymbol{\rho}_s). \tag{68}$$

Therefore, the necessary and sufficient conditions for stability can be obtained with the use of the $L - S - V$ coefficients in exactly the same way as it has been done in Section 3. Namely, the stability conditions are given by (14–16), with the forces modified by (68).

https://doi.org/10.1017/S0263574799002465 Published online by Cambridge University Press

Let us revisit the example from Section 5 and assume $k_{pi} = k_p$, $i = 1, \ldots, 4$, so that the stiffness center coincides with the geometric center of the contact points. Calculation of L gives $L = L_0 + k_p L_1$, where L_0 takes the form of (54) and $L_1 = 4(a^2 \cos^{\frac{4}{m}} \psi + b^2 \sin^{\frac{4}{m}} \psi)$. The stability condition is $k_p > -L_o/L_1$. The minimal stable gain, normalized with respect to $f_n/\sqrt{ab}$, is a function of the grasping angle ψ and the normalized tangential force f_t/f_n. This function is plotted in Figure 13 for $a = b$.

In the case of sphere ($m = 2$), for which the force distribution (52) is unstable, calculation of L gives $L = 4a(ak_p - f_n)$ and the stability condition is stated as $k_p > f_n/a$. This condition does not depend on ψ and f_t, and therefore the normalized minimal gain surface for $m = 2$ is flat at the unit level.

Next, considering the stability condition at the critical angle (55), one gets

$$k_p > f_n \sin^{1-\frac{2}{m}} \psi / b = f_n \cos^{1-\frac{2}{m}} \psi / a. \tag{69}$$

As can be seen, k_p increases indefinitely as $m \to 0$ while it is limited when $m \to \infty$. The reason is not related to the curvature, which goes to infinity as $m \to 0$ or $m \to \infty$, and is in the fact that the distance between the contact points goes to zero as $m \to 0$.

If the grasping takes place in three dimensions, one must consider the second condition, $S > 0$. Calculation of S gives $S = k_p^2 S_2 + k_p S_1 + S_0$, where S_0 takes the form of (59), $S_2 = 16a^2b^2 \cos^{\frac{4}{m}} \psi \sin^{\frac{4}{m}} \psi$, and

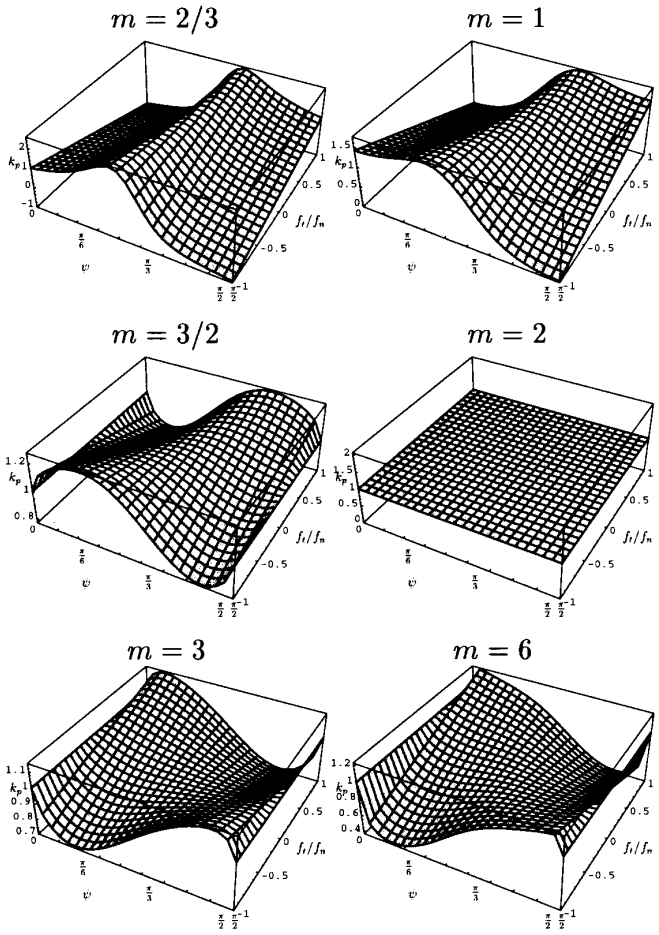

Fig. 13. Normalized minimal stable gain coefficient.

$$S_1 = -\frac{16ab \cos^{\frac{2}{m}} \psi \sin^{\frac{2}{m}} \psi}{\lambda(\psi)} \Big(f_t\, ab \cos 2\psi \cos^{\frac{2}{m}} \psi \sin^{\frac{2}{m}} \psi$$

$$+ f_n (a^2 \cos^{\frac{4}{m}} \psi \sin^2 \psi + b^2 \sin^{\frac{4}{m}} \psi \cos^2 \psi) \Big). \tag{70}$$

The values of k_p satisfying $S > 0$ belong to the following interval:

$$k_p \in (-\infty, \min\{k_1, k_2\}), \cup\ (\max\{k_1, k_2\}, \infty), \tag{71}$$

where

$$k_1 = \frac{1}{\lambda(\psi)} \Big(\frac{b}{a} f_n \cos^2 \psi \tan^{\frac{2}{m}} \psi - f_t \sin^2 \psi \Big), \tag{72}$$

$$k_2 = \frac{1}{\lambda(\psi)} \Big(\frac{a}{b} f_n \sin^2 \psi \cot^{\frac{2}{m}} \psi + f_t \cos^2 \psi \Big). \tag{73}$$

Considering the conditions $L > 0$ and $S > 0$ together, it can be shown that for a given f_t/f_n there exists a point ψ where $k_1 = k_2 = -L_0/L_1$. At this point the condition $k_p > -L_0/L_1$ cuts the interval (71) so that the spatial stability condition takes the form $k_p > \max\{k_1, k_2\}$. For example, in the case of sphere one obtains

$$\begin{cases} k_p > (f_n + f_t \cot \psi)/a, & \text{if } f_t > 0, \\ k_p > (f_n - f_t \tan \psi)/a, & \text{if } f_t < 0. \end{cases} \tag{74}$$

One can see that as $\psi \to 0$ or $\psi \to \pi/2$, that is when the four contact points are degenerating to the two contact points, more and more higher gain coefficients k_p are required to stabilize the grasp. However, unlimited increase of k_p may result in slip and loss of equilibrium.

7. COMMENT ON THE CONTACT STABILITY

The grasp under the control (61) with properly adjusted k_p and k_v can be made asymptotically stable. However, it is not always globally asymptotically stable. The area of its asymptotical stability in the space of the object disturbances is limited by the unilateral constraints

$$|(\boldsymbol{n}_i + \Delta\boldsymbol{n}_i) \times (\boldsymbol{f}_i + \Delta\boldsymbol{f}_i)| \le \mu\{(\boldsymbol{f}_i + \Delta\boldsymbol{f}_i) \cdot (\boldsymbol{n}_i + \Delta\boldsymbol{n}_i)\}. \tag{75}$$

The correction $\Delta\boldsymbol{f}_i$, not violating the object contact stability, must belong to the friction cone (75) whose origin is shifted along the vector $\boldsymbol{f}_i$. Here one comes to the notion of the contact stability[27] as opposed to the object stability.

To define the contact stability area in the space of the object disturbances, one represents $\Delta\boldsymbol{n}_i$ and $\Delta\boldsymbol{x}_i$ with the use of Rodrigues' formula for the finite rotations,

$$\Delta\boldsymbol{n}_i = \sin\theta(\boldsymbol{k} \times \boldsymbol{n}_i) + (1 - \cos\theta)\{\boldsymbol{k} \times (\boldsymbol{k} \times \boldsymbol{n}_i)\} \tag{76}$$

$$\Delta\boldsymbol{x}_i = \sin\theta(\boldsymbol{k} \times \boldsymbol{\rho}_i) + (1 - \cos\theta)\{\boldsymbol{k} \times (\boldsymbol{k} \times \boldsymbol{\rho}_i)\} + \Delta\boldsymbol{x}, \tag{77}$$

and solves the system of inequalities (75) with respect to $\Delta\boldsymbol{x}$ and $\theta\boldsymbol{k}$. Here, θ is the disturbance angle, and $\boldsymbol{k}$ stands for the disturbance axis.

In general, the solution of (75) is quite complicated and can be done only numerically. In the rest of the section we complete the example considered earlier and show how the

https://doi.org/10.1017/S0263574799002465 Published online by Cambridge University Press

upper bounds for k_p are established for the cases of pure rotational and pure translational disturbances. Assume $\boldsymbol{k} = \{0, 0, 1\}^{\mathrm{T}}$. Several simple but instructive conclusions can be drawn from this example.

Linear disturbances. Let $\theta = 0$. The system of inequalities (75) takes the following form

$$| \boldsymbol{k} f_t - k_p(\boldsymbol{n}_i \times \Delta \boldsymbol{x}) | \leq \mu \{ f_n - k_p(\boldsymbol{n}_i \cdot \Delta \boldsymbol{x}) \}. \tag{78}$$

It can be shown that (78) satisfies $\forall i = 1, \ldots, 4$ if

$$| \Delta \boldsymbol{x} | \leq \frac{\mu f_n - | f_t |}{k_p(1 + \mu)}. \tag{79}$$

On the other hand, if

$$| \Delta \boldsymbol{x} | > \frac{\mu f_n + | f_t |}{k_p(1 - \mu)}, \tag{80}$$

the system (78) has no solution. As can be seen, increasing k_p decreases the size of the contact stability area. It can be viewed as the contradiction between the Liapunov stability and the contact stability of the object.

For the grasp to be both Lyapunov stable and contact stable, the upper bound for k_p, defined from (79), should be compatible with the lower bound given by the Liapunov stability considerations. Consider the case of sphere for which $k_p > f_n/a$. Let $f_t = 0$. The compatibility will be guaranteed if $| \Delta \boldsymbol{x} | < a\mu/(1 + \mu)$. For example, for $\mu = 0.2$ and $a = 10$cm the grasp can be made both Liapunov stable and contact stable if, roughly, $| \Delta \boldsymbol{x} | < 1.6$cm. On the other hand, if $| \Delta \boldsymbol{x} | > a\mu/(1 - \mu)$, that is $| \Delta \boldsymbol{x} | > 2.5$cm in our example, the contact stability will be violated.

Note that the estimates (79) and (80) can be very rough since they do not depend on the specific shape of the object and on the grasping angle. To illustrate this point, consider the exact area of admissible disturbances. The area is represented by intersection of two rhombuses whose orientation depends on the grasping angle ψ. The intersection area is depicted in Figure 14 for $f_t = 0$ and $\psi = \pi/4$. It can be shown that for $f_t = 0$ and $\psi = \pi/4$ the circle inscribed into the contact stability area is defined as $| \Delta \boldsymbol{x} | < a\mu$, which gives $| \Delta \boldsymbol{x} | < 2.0$cm for $\mu = 0.2$ and $a = 10$cm.

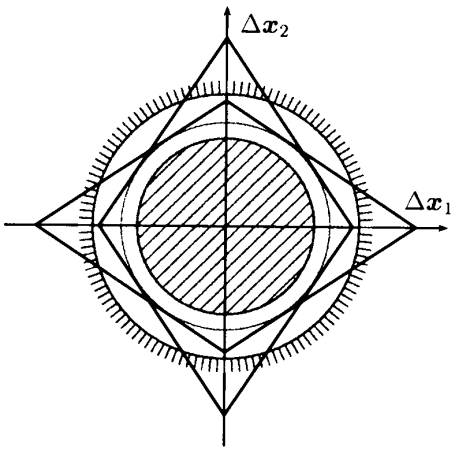

Fig. 14. No-slip translational disturbances.

Rotational disturbance. Let $\Delta \boldsymbol{x} = \boldsymbol{0}$. The system of inequalities (75) takes the following form

$$\begin{aligned} &| (k_p \lambda_n - f_n) \sin\theta + f_t \cos\theta - k_p \lambda_t (1 - \cos\theta) | \\ &\leq \mu \{ (k_p \lambda_t + f_t) \sin\theta + f_n \cos\theta + k_p \lambda_n (1 - \cos\theta) \}, \end{aligned} \tag{81}$$

where

$$\lambda_n = \frac{ab \cos^{2/m}\psi \sin^{2/m}\psi}{\lambda(\psi)}, \tag{82}$$

$$\lambda_t = \frac{a^2 \cos^{4/m}\psi \sin^2\psi - b^2 \sin^{4/m}\psi \cos^2\psi}{\lambda(\psi)}. \tag{83}$$

Consider the configuration corresponding to the critical grasping angle (55) for which $\lambda_t = 0$. If there is no tangential force ($f_t = 0$) and k_p is set to be on the boundary of the Liapunov stability condition for the coefficient $L(k_p = f_n/\lambda_n)$, the inequality (81) will be satisfied for relatively large disturbances such that $|\theta| < \pi/2$. A direct consequence of this fact is that for $f_t = \lambda_t = 0$ and $|\theta| < \pi/2$ the upper bound for k_p will be always compatible with the lower bound, defined from the Liapunov stability considerations. For example, in the case of sphere (for which any ψ is critical) and small θ one gets $k_p < f_n(1 + \mu/|\theta|)/a$.

CONCLUSIONS

The problem of the stability of a rigid body subjected to multiple frictional contacts has been considered in this paper. First, the stability of a force distribution was formulated at the level of force planning. For this subproblem the stiffness tensor of the system has been derived, and its basic properties has been established. Necessary and sufficient conditions for stability of a force distribution have been established in an analytical form in terms of the so-called $L - S - V$ coefficients. These conditions, considered under unilateral frictional constraints, have been studied on an illustrative example.

Next, at the level of the feedback stabilization, it has been shown that an unstable force distribution can be stabilized by a simple control law. The stability conditions for this control law have been formulated in terms of the original stiffness tensor and the stiffness tensor of the "control" springs calculated at the stiffness center. The stability conditions can be defined with the use of the $L - S - V$ coefficients, with the contact forces modified by the elastic forces of the "control" springs. Finally, conclusions on the relation between the Liapunov stability and the contact stability of the objects have been drawn.

References

1. K. Shimoga, "Robot grasp synthesis algorithms: A survey", *Int. J. Robotics Research* **15**(3) 230–266 (1996).
2. I. Walker, "Multi-fingered hands: A survey", **In**: *Complex Robotic Systems. Lecture Notes in Control and Information Sciences*, (P. Chiacchio and S. Chiaverini, Eds.) (Vol. 233, Springer-Verlag, 1998) pp. 129–160.
3. N. Brook, M. Shoham and J. Dayan, "Controlability of grasps and manipulations in multi-fingered hands", *IEEE Trans. on Robotics and Automation* **14**(1) 185–192 (1998).

https://doi.org/10.1017/S0263574799002465 Published online by Cambridge University Press

4. H. Hanafusa and H. Asada, "Stable prehension by a robot hand with elastic fingers", **In:** *Robot Motion: Planning and Control* (M. Brady, J. Hollerbach, T. Johnson, T. Lozano-Perez and M. Mason; Eds.) (MIT Press, Camridge, USA, 1982) pp. 323–336.
5. M. Cutkosky and I. Kao, "Computing and controlling the compliance of a robot hand", *IEEE Trans. on Robotics and Automation* **5**(2) 151–165, (1989).
6. V.-D. Nguyen, "Constructing stable grasps" *Int. J. Robotics Research* **8**(1) 26–37, (1989).
7. M. Kaneko, N. Imamura, K. Yokoi and K. Tanie, "A Realization of stable grasp based on virtual stiffness model by robot fingers", *Proc. IEEE Int. Workshop on Advanced Motion Control*, Yokohama, Japan (1990) pp. 156–163.
8. H. Maekawa, "Stable grasp and manipulation of 3D object by multifingered hands", *Proc. 2nd Int. Symp. on Measurement and Control in Robotics, ISMCR'92*, Tsukuba, Japan (1992) pp. 335–341.
9. H.-R. Choi, W.-K. Chung and Y. Youm, "Stiffness analysis and control of multi-fingered robot hands", *Trans. ASME, Journal of Dynamic Systems, Measurement and Control* **117**(3) 435–439 (1995).
10. D. Montana, "Contact stability for two-fingered grasps", *IEEE Trans. on Robotics and Automation* **8**(4) 421–430 (1992).
11. W. Howard and V. Kumar, "Stability of planar grasps", *Proc. IEEE Int. Conf. on Robotics and Automation*, San Francisco, USA (1994) pp. 2822–2827.
12. H. Maekawa, K. Tanie and K. Komoriya, "Kinematics, statics and stiffness effect of 3D grasp by multifingered hand with rolling contact at the fingertip", *Proc. IEEE Int. Conf. on Robotics and Automation*, Albuquerque, USA (1997) pp. 78–85.
13. Q. Lin, J. Burdick and E. Rimon, "Computation and analysis of compliance in grasping and fixturing", *Proc. IEEE Int. Conf. on Robotics and Automation*, Albuquerque, USA (1997) pp. 93–99.
14. R. Mason, E. Rimon and J. Burdick, "The stability of heavy objects with multiple ontacts", *Proc. IEEE Int. Conf. on Robotics and Automation*, Nagoya, Japan (1995) pp. 439–445.
15. M. Cutkosky, *Robotic Grasping and Fine Manipulation* (Kluver Academic Publishers, Boston, 1985).
16. H. Hanafusa and M. Adli, "Effect of internal forces on stiffness of closed mechanisms", *Proc. 5th Int. Conf. on Advanced Robotics*, Pisa, Italy (1991) pp. 845–850.
17. B. Yi, D. Tesar and R. Freeman, "Geometric stability in force control", *Proc. IEEE Int. Conf. on Robotics and Automation*, Sacramento, USA (1991) pp. 281–286.
18. F. Jen, M. Shoham and R. Longman, "Liapunov stability of forced-controlled grasps with a multi-fingered hand", *Int. J. Robotics Research* **15**(2) 137–154 (1996).
19. J. Broida and S. Williamson, *A Comprehensive Introduction to Linear Algebra* (Addison-Wesley, New York, 1989).
20. R. Bellman, *Introduction to Matrix Analysis* (McGraw-Hill, New York, 1960).
21. A. Ben-Israel and T. Greville, *Generalized Inverses: Theory and Application* (Wiley, New York, 1974).
22. V. Kumar and K. Waldron, "Force distribution in closed kinematic chains", *IEEE Journal of Robotics and Automation* **4**(6) 657–664 (1989).
23. R.G. Bonitz and T. Hsia, "Force decomposition in cooperating manipulators using the theory of metric spaces and generalized inverses", *Proc. IEEE Int. Conf. on Robotics and Automation*, San Diego, USA (1994) pp. 15231–1527.
24. D. Williams and O. Khatib, "Characterization of internal forces in multi-grasp manipulation", *Proc. 2nd Int. Symp. on Measurement and Control in Robotics, ISMCR'92*, Tsukuba, Japan (1992) pp. 731–738.
25. T. Yoshikawa, "Virtual truss model for characterization of internal forces for multiple finger grasps", *Proc. IEEE Int. Conf. on Robotics and Automation*, Leuven, Belgium (1998) pp. 2389–2395.
26. R. Horn and C. Johnson, *Matrix Analysis* (Cambridge University Press, Cambridge, 1986).
27. Y. Nakamura, K. Nagai and T. Yoshikawa, "Dynamic and stability in coordination of multiple robotic mechanisms", *Int. J. Robotics Research* **8**(2) 44–61 (1989).

https://doi.org/10.1017/S0263574799002465 Published online by Cambridge University Press